Composites Part B 185 (2020) 107797

Contents lists available at ScienceDirect

Composites Part B

journal homepage: www.elsevier.com/locate/compositesb

A facile and efficient flame-retardant and smoke-suppressant resin coating for expanded polystyrene foams

Meng-En Li, Yuan-Wei Yan, Hai-Bo Zhao *, Rong-Kun Jian, Yu-Zhong Wang **

Collaborative Innovation Center for Eco-Friendly and Fire-Safety Polymeric Materials (MoE), State Key Laboratory of Polymer Materials Engineering, National Engineering Laboratory of Eco-Friendly Polymeric Materials (Sichuan), College of Chemistry, Sichuan University, Chengdu, 610064, China

ARTICLE INFO

Keywords:
Coating
Expanded polystyrene foam
Flame retardancy
Smoke suppression

ABSTRACT

Flame-retardant and smoke-suppressant expanded polystyrene (EPS) foams were prepared by coating a mixture of thermoplastic phenolic resin (PF) and aluminum hypophosphite (AP) or expandable graphene (EG) onto EPS spheres. The PF reacting with AP by hydrogen-bond interaction formed a facile flame-retardant coating PF/AP, which not only greatly reduced flammability and smoke release, but also remained the thermal conductivities of EPS foams at low level. Compared with those of EPS/PF/EG, EPS/PF/AP could pass the UL-94 test and showed better flame-retardant performances with lower heat release rates and fire growth rates. Especially, the time to ignition (TTI) of EPS/PF/AP achieved 52 s, much higher than those of EPS/PF/EG (9 s) and neat EPS (2 s). Also, the peak of smoke production rate (PSPR) and the total smoke production (TSP) of both composites were significantly reduced, showing an excellent smoke-suppressant performance. The mechanism analysis suggested that the PF/AP coating could form a compact P–O–C cross-linked char layer and effectively protect the matrix from further combusting. Particularly, the EPS/PF/AP had a higher compressive strength and lower thermal conductivity in comparison with EPS/PF/EG. These above results show that the EPS/PF/AP composite has enormous potential in building thermal insulation field.

1. Introduction

EPS foam is widely used in packaging, appliances, building insulations, and decorations because of its outstanding properties, such as superior thermal insulation, excellent dimensional stability, low cost, low density, and low sensitivity to moisture, and occupies the largest market share in building insulation materials [1–4]. However, it's extremely flammable due to its high air content (98%) and porosity, and concerns for the fire safety of the EPS foam have grown greatly nowadays. Also, EPS will produce lots of toxic smoke during burning, which is regarded as the leading death cause in a fire. Therefore, it's of vital importance to improve the flame retardancy and smoke suppression of EPS.

From the 1960s to 1980s, the introduction of brominated flame retardants, such as tetrabromoethane and hexabromocyclododecane, had been commercially developed to solve the potential safety problems related to fire hazard of EPS [5–7]. Bromine, due to its low bonding energy with carbon atoms, could be readily released and took part in the burning process by quenching the free-radicals in the gas phase [8,9]. However, in the 1990s, it was discovered that the halogenated products would affect the human health and the environment [10,11]. So, it's urgent that new flame-retardant systems instead of halogenated substances should be developed to meet the constantly changing demand of new regulations and standards [12–15].

Halogen-free flame retardants are eco-friendlier compared with the halogenated ones [16–18]. However, a large amount of halogen-free flame retardants should be added into EPS during the polymerization or impregnation process because of its low flame-retardant efficiency, which will largely deteriorate the mechanical properties and other intrinsic qualities of the foam. In the circumstances, coating the flame retardants onto EPS beads might be a good option, which has little effect on the foaming process [5].

Flame-retardant coatings [19,20], composed of adhesive and flame retardant, have been widely utilized to endow EPS with flame retardancy. The thermosetting PF, due to its inherent fire resistance and excellent adhesion, is usually used as an adhesive [21]. And EG is the most common halogen-free flame retardant owing to its great flame retardancy. It was reported that the incorporation of 15 wt% EG made

* Corresponding author.
** Corresponding author.
E-mail addresses: haibor7@163.com (H.-B. Zhao), polymers@vip.126.com (Y.-Z. Wang).

https://doi.org/10.1016/j.compositesb.2020.107797
Received 30 August 2019; Received in revised form 4 December 2019; Accepted 19 January 2020
Available online 22 January 2020

EPS pass the German standard for building materials DIN 4102 with a B2 rating [22]. However, EG has comparative large dimension, leading to poor dispersion and compatibility in adhesives. What's more, EG restrains the combustion by expanding to several times bigger, while the adhesive often cannot expand. As a result, the residual char is non-compact with large crack, resulting in relatively poor flame-retardant efficiency, such as failing to pass the UL-94 tests. Although co-addition of triphenyl phosphate, red phosphorus and chalk helped to further improve the flame-retardant efficiency, the smoke production was increased [23,24]. The smoke suppression for EPS is still a big challenge.

Therefore, it is of significance to find an effective eco-friendly flame-retardant and smoke-suppressant method for EPS. Recently, AP has attracted a lot of researchers' attention because of its low cost and high efficiency [25,26]. Also, there are many hypophosphite groups in AP, which could form hydrogen bond with PF, leading to a better compatibility. Therefore, in this manuscript, to further improve the flame retardancy and smoke suppression of EPS foam, AP was utilized as the flame retardant to react with PF and EPS/PF/AP composite was fabricated for the first time. And we compared the flame retardancy and smoke suppression of the EPS/PF/AP with EPS/PF/EG composites, and investigated the different flame-retardant and smoke-suppressant mechanisms of PF/AP and PF/EG coating on EPS in detail.

2. Experimental

2.1. Materials

EPS beads were purchased from Jiangyin Nijiaxiang New Material Co., Ltd (Jiangyin, China). AP was prepared according to the previous literature [27]. EG (diameter: 180 μm, and expansion ration: 230) was purchased from Shijiazhuang ADT Carbonic Material Factory (ADT 802, Shijiazhuang, China). Hexamethylene tetramine and ethanol were provided by Kelong Chemical Reagent Company (Chengdu, China). Thermoplastic phenolic resin (PF) was purchased from Chengdu Changzheng Glass Co., Ltd (Chengdu, China).

2.2. Samples preparation

Firstly, EPS beads were heated at 98 °C for 15–20 min, and then the pre-foamed PS beads were stored for 24 h before the next step. Secondly, the flame retardant (EG or AP) and curing agent (Hexamethylene tetramine) were mixed with thermoplastic PF, which was dissolved in a certain amount of ethanol at room temperature, to prepare the flame-retardant coating. At last, the pre-foamed PS beads were well mixed with flame-retardant coating, following by being introduced into a mold and treated at 105 °C and a certain pressure for 8 min. The products were fully cured at 60 °C for 2 days and cut into standard testing bars. The preparation route of the EPS/PF/AP composites was shown in Scheme 1 and the specific formulations of EPS composites were listed in Table 1.

2.3. Measurement

The density of EPS composites was calculated by the average values of five samples larger than 100 cm^3, according to ISO 845: 2006.

The LOI values were measured by an HC-2C oxygen index meter (Jiangning, China) according to ASTM D2863-97 and the dimension of all samples was 150 mm × 12.5 mm × 12.5 mm.

The UL-94 test was performed on a CZF-2 instrument (Jiangning, China) according to ASTM D3801 and dimension of all samples was 250 mm × 20 mm × 20 mm.

The CC tests were conducted according to ASTME 1354/ISO 5660-1 (Fire Testing Technology, UK) at a heat flux of 25 kW/m^2. The size of samples was cut into 100 mm × 100 mm × 20 mm.

The mechanical properties were determined by an electronic universal testing machine (Instron, USA) at 2 mm/min rate according to ISO 844: 2004. The compressive strength was the average of at least five individual measurements and dimension of all samples was 50 mm × 50 mm × 20 mm.

The thermal conductivity of EPS composites was measured by Hot Disk 2500-OT (Hot Disk, Sweden) in accordance with ISO22007-2:2008. The size of the specimen was 30 mm × 30 mm × 10 mm.

The morphologies of the char residues collected after the cone calorimeter tests were observed using scanning electron microscopy

Table 1
The specific formulations of EPS and its composites.

Sample	EPS (g)	PF (g)	Curing agent (g)	AP (g)	EG (g)
EPS	6.5	-	-	-	-
EPS/10 PF	6.5	10	1.11	-	-
EPS/10PF/3 EG	6.5	10	1.11	-	3
EPS/10PF/1AP	6.5	10	1.11	1	-
EPS/10PF/2AP	6.5	10	1.11	2	-
EPS/10PF/3AP	6.5	10	1.11	3	-
EPS/5PF/3 EG	6.5	5	0.56	-	3
EPS/5PF/3AP	6.5	5	0.56	3	-

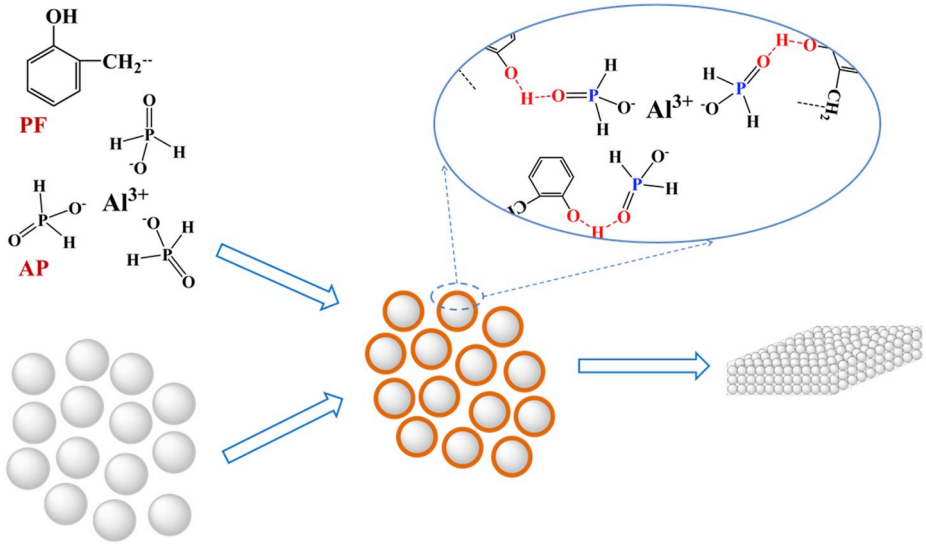

Scheme 1. The fabrication route for EPS/PF/AP composites.

(JEOL JSM 5900LV).

X-ray photoelectron spectroscopy (XPS) spectra were obtained by a XSAM80 (Kratos Co., UK), with an Al Kα excitation radiation (hv-1486.6 eV).

Raman spectroscopy measurement was carried out at room temperature with LabRAM HR800 laser Raman spectrometer (SPEX Co., USA) by a 532 nm helium-neon laser line.

3. Results and discussion

3.1. Flammability of EPS composites

3.1.1. LOI and UL-94 tests

The LOI and vertical burning tests (UL-94) were carried out at room temperature to investigate the small fire safety of the EPS composites. And the detailed data were listed in Table 2. Neat EPS showed a high flammability with a very low LOI value (17.0%) and failed to pass UL-94 rating. In addition, it exhibited serious shrinkage and melt-dripping during burning. EPS/10 PF had an increased LOI value of 21.0% but still had no UL-94 rating. With the incorporation of AP or EG, the LOI values of EPS/10PF/3AP and EPS/10PF/3 EG were obviously increased to 28.0% and 29.0%, and the UL-94 ratings of the composites were V-0 and V-1, respectively. To reduce the density of the foam, EPS/5PF/3AP (52 kg/m^3) and EPS/5PF/3 EG (50 kg/m^3) were prepared. The LOI value of EPS/5PF/3AP was 27.5% and the UL-94 rating was V-0 rating. However, EPS/5PF/3 EG with LOI value of 28.0% had no rating in the UL-94 test. These results indicated the flame retardancy of EPS was improved greatly with the flame-retardant PF/AP or PF/EG coating. What's more, AP exhibits better flame-retardant efficiency than EG.

3.1.2. Cone calorimetric analysis

Cone calorimetry is one of the most widely used techniques to evaluate the flammability of polymeric materials. The combustion environment in the CC test is similar to the real scale fire, so the results of the cone calorimeter can evaluate the real fire performance of the materials [28–31]. The detailed cone calorimetric parameters of EPS and its composites at an incident heat flux of 25 kW/m^2 are listed in Table 3, including the time to ignition (TTI), the peak of heat release rate (PHRR), the time to PHRR (t_p), the average heat release rate (av-HRR), the mass loss rate (MLR), the peak of smoke production rate (PSPR), and the total smoke production (TSP).

As shown in Table 3, neat EPS was very easy to be ignited with TTI of 2 s. Even when coated by PF/EG, the material showed a considerably low TTI of 9 s. On the contrary, the TTI value of the EPS/PF/AP composite was increased by a large extent, owing to the introduction of AP-containing coatings. Especially for EPS/10PF/3AP, the TTI was as high as 52 s, which was 25 times higher than that of neat EPS (2 s). It was indicated that the PF/AP coating covered the substance to prevent it to be ignited effectively.

Fig. 1 shows the HRR curves for neat EPS and flame-retardant EPS composites. It was notable that PHRR and av-HRR, which were recognized as the most important factors in controlling the fire hazard, were obviously reduced. The PHRR value of neat EPS was 286 kW/m^2, while EPS/10PF/3 EG and EPS/10PF/3AP had much lower PHRR value of 124 and 115 kW/m^2, respectively. The av-HRR values of EPS/10PF/3 EG and EPS/10PF/3AP were 71 and 61 kW/m^2, respectively, much lower than that of neat EPS (196 kW/m^2). These results indicated the coatings with either EG or AP could restrain the fire intensity of EPS. The fire growth rate (FIGRA) could be calculated through PHRR/t_p to assess the fire hazards of the composites [32]. Low FIGRA value indicated delayed time to flashover, which allowed enough time to evacuate and for fire extinguishers to arrive [33]. The FIGRA value of EPS/10PF/3 EG was decreased from 4.8 to 2.5 kW m-2s^{-1} compared to that of neat EPS, and EPS/10PF/3AP exhibited the lowest FIGRA value of 1.5 kW/m^2·s. The obvious reduction of FIGRA values suggested that the coated EPS burnt with a lower propensity compared to the neat EPS.

Table 2
The densities, LOI and UL-94 tests results of EPS and its composites.

Sample	Density (kg/m^3)	LOI (%)	UL-94
EPS	24	17.0	NR
EPS/10 PF	58	21.0	NR
EPS/10PF/3 EG	67	29.0	V-1
EPS/10PF/1AP	59	23.0	V-2
EPS/10PF/2AP	61	25.0	V-2
EPS/10PF/3AP	66	28.0	V-0
EPS/5PF/3 EG	50	28.0	NR
EPS/5PF/3AP	52	27.5	V-0

Fig. 2 gives the mass loss rate curves of EPS and its composites. At the end of the CC test, there were 0, 51 and 63 wt% of char residues left for neat EPS, EPS/10PF/3 EG and EPS/10PF/3AP, respectively. The figure showed that the coatings enhanced the burning residues of the composites and decreased the mass loss rate markedly. The mass loss rate of neat EPS was 0.066 g/s (shown in Table 3). When the flame-retardant coating with EG or AP was introduced to EPS, it was decreased to 0.022 g/s and 0.021 g/s, respectively. The results indicated that the flame-retardant coatings played an important role in restraining the combustion of the composites.

Smoke production in the fire is one of the most important factors, which directly causes people to death by suffocation and/or inhalation of the toxic gases [34]. Table 3 and Fig. 3 clearly show the smoke emission behaviors of all composites under an external heat flux of 25 kW/m^2. Both PF/AP and PF/EG coatings could slow down the SPR and reduced PSPR from 0.132 m^2/s of neat EPS to 0.046 and 0.063 m^2/s, respectively. It was notable that EPS/10PF/3AP had a little higher PSPR value compared to EPS/10PF/3 EG, which was different from their other data such as TSP, PHRR, MLR, etc. The reason might be that AP released a certain amount of gas species during the combustion [26]. TSP value greatly decreased from 7.00 m^2 of neat EPS to 4.04 m^2 of EPS/10PF/3 EG and 3.21 m^2 of EPS/10PF/3AP, respectively. The great reduction in PSPR and TSP showed that the flame-retardant coatings could suppress the smoke effectively, which would significantly increase the chances of people escaping in a fire.

To sum up, the flame-retardant coatings with EG or AP can greatly improve the flame retardancy and the smoke suppression of EPS and the coating with AP has better integrated flame retardancy. To investigate the different performance of the two coatings, their flame-retardant and smoke-suppressant mechanisms were studied as follows.

3.2. Flame-retardant and smoke-suppressant mechanisms

3.2.1. Analysis of the char residue of EPS composites

Fig. 4 gives the digital photos of the residue of EPS/10 PF, EPS/10PF/3 EG and EPS/10PF/3AP after the CC tests (EPS had no residue left). It was observed that the residues for EPS/10PF/3 EG and EPS/10PF/3AP remained the original shape of the specimen after the tests while that of EPS/10 PF had little char left with lots of holes (Fig. 4a, d), which indicated that the PF/AP and PF/EG coatings could prevent the shrinkage of the materials by forming stable char residue. EPS/10PF/3 EG had an intumescent char layer because EG could expand to hundreds of times larger than the former dimension during combustion. But the crack between char residues was large, which resulted in loose char layer (Fig. 4e). On the contrary, EPS/10PF/3AP had a more compact char layer (Fig. 4f). It is known that the char layer can act as a physical barrier which can slow down heat and mass transfer between burning zone and polymer matrix beneath [35]. The SEM images for residues of EPS/10PF/3 EG and EPS/10PF/3AP further showed that EPS/10PF/3AP had more compact char layer, which was the reason why it had much lower PHRR, MLR, TSP, etc.

3.2.2. Raman spectroscopy of the char residue

To further characterize the char residues of EPS/10PF/3 EG and EPS/

Table 3
Cone calorimetric data for EPS and its composites.

Sample	TTI (s)	PHRR (kW/m^2)	t_p (s)	FIGRA[a] (kW/m^2·s)	Av-HRR (kW/m^2)	MLR (g/s)	PSPR (m^2/s)	TSP (m^2)
EPS	2	286	60	4.8	196	0.066	0.132	7.00
EPS/10 PF	3	191	60	3.2	137	0.043	0.135	7.60
EPS/10PF/3 EG	9	124	50	2.5	71	0.022	0.046	4.04
EPS/10PF/3AP	52	115	75	1.5	61	0.021	0.063	3.21

[a] FIGRA is calculated by dividing the peak HRR by the time to PHRR.

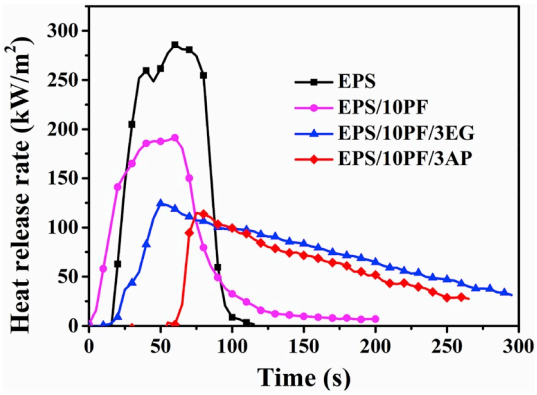

Fig. 1. Heat release rate (HRR) curves for EPS, EPS/10 PF, EPS/10PF/3 EG and EPS/10PF/3AP under an external heat flux of 25 kW/m^2.

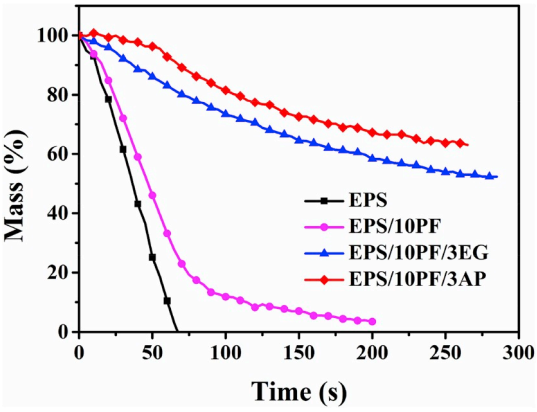

Fig. 2. The mass loss rate curves for EPS, EPS/10 PF, EPS/10PF/3 EG and EPS/10PF/3AP under an external heat flux of 25 kW/m^2.

10PF/3AP, Raman spectroscopy was used, which can characterize the different types of carbonaceous materials, particularly for the carbonaceous materials formed during combustion [36,37]. Fig. 5 shows the Raman spectra for the char residue of EPS/10 PF/EG and EPS/10PF/3AP after CC tests. It shows both the testing samples' spectra exhibit overlapping peaks with intensity maxima at about 1580 cm^{-1} and 1360 cm^{-1}. The first band (the G band) is corresponding to the stretching vibration mode with E_{2g} symmetry in the sp^2 hybridized carbon atoms in a graphite layer, whereas the latter one (the D band) represents disordered graphite or glassy carbons [38]. More importantly, according to the research of Tuinstra and Koening, the relative ratio of the integrated intensities of D and G band (A_D/A_G) is inversely proportional to an in-plane microcrystalline size, where A_D and A_G are the integrated intensities of D and G bands, respectively [39,40]. Basically, the bigger ratio of A_D/A_G is, the smaller size of carbonaceous microstructures is, which means more compact microstructure [41,42]. Fig. 5 showed that the A_D/A_G ratio of EPS/10PF/3AP was much bigger than that of EPS/10PF/3 EG, indicating that the PF/AP coating had more compact carbonaceous microstructure. It is consistent with the results of SEM images and digital photos.

3.2.3. XPS analysis

XPS for the char residues of EPS/10 PF/EG and EPS/10PF/3AP after CC tests was utilized to study the atomic concentration of carbon (C), oxygen (O), phosphorus (P) and aluminum (Al). Table 4 shows the element concentration of C, Al, O and P tested by XPS. For EPS/10PF/3 EG, the main element of the residue was C (92 wt%) while a lot of P (7.8 wt%), O (18.4 wt%) existed in the residue for EPS/10PF/3AP. That was to say, many P and O took part in the charring process to form P–O–C cross-linked char layer, which prevented the matrix from further combusting. This result is in accordance with the results of SEM and Raman.

Combining the above tests with some previous literatures [25,26], the possible flame-retardant and smoke-suppressant mechanisms of different coatings are proposed as Scheme 2: For EPS/PF/EG, when the composite is exposed to the fire, the coating begins to be carbonized quickly and form a char layer which acts as an isolating layer between the fire and matrix. EG can expand to hundreds of times larger than the former dimension during the combustion, but PF cannot expand, as a result, the crack between char residue is large, and the char layer is loose. As for EPS/PF/AP, during combustion, the PF/AP coating can be carbonized to be a P–O–C cross-linked char layer, which has better carbonaceous microstructure compared to PF/EG. The compact char layer can protect the matrix from further combusting. Meanwhile, AP

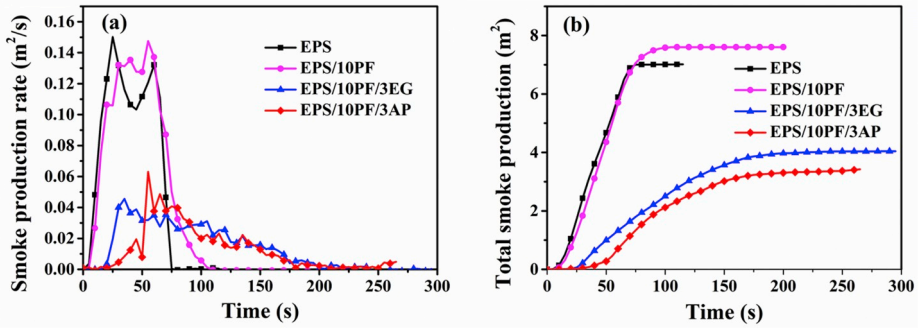

Fig. 3. Smoke production rate (SPR, a) and total smoke production (TSP, b) curves for EPS, EPS/10 PF, EPS/10PF/3 EG and EPS/10PF/3AP under an external heat flux of 25 kW/m^2.

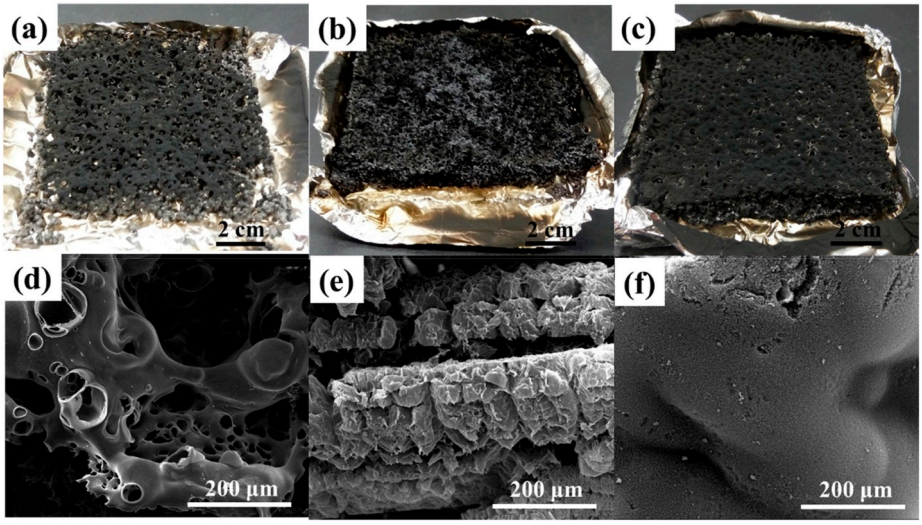

Fig. 4. Digital photographs and SEM images for the residue char after CC tests: digital photographs for EPS/10 PF (a), EPS/10PF/3 EG (b), and EPS/10PF/3AP (c); SEM image for EPS/10 PF (d), SEM image for EPS/10PF/3 EG (e), and SEM image for EPS/10PF/3AP (f).

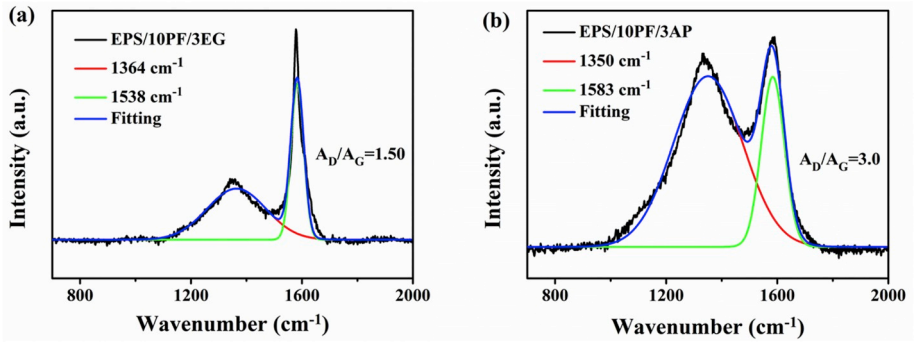

Fig. 5. Raman spectra for the char residues of EPS/10PF/3 EG and EPS/10PF/3AP after CC tests.

Table 4
The element concentration of C, Al, O and P under XPS tests.

Sample	C (wt %)	Al (wt %)	O (wt %)	P (wt %)
EPS/10PF/3 EG	92.0	-	7.6	0.4
EPS/10PF/3AP	70.9	2.9	18.4	7.8

can generate PO2- in the degradation products to exhibit a gas-phase activity [25,26], which can improve the flame retardancy and smoke suppression of the material in the combustion.

3.3. Mechanical and thermal insulation properties of EPS composites

3.3.1. Mechanical properties

Compressive strength is the most important mechanical property for polymer foams, and the corresponding data of EPS, EPS/10PF/3 EG and

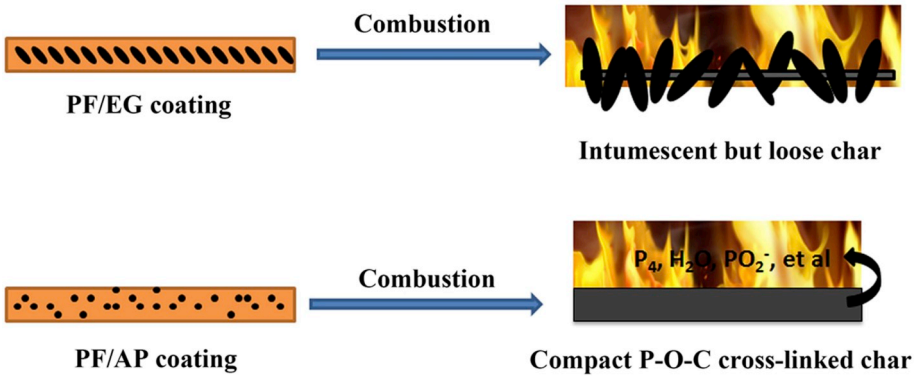

Scheme 2. The possible flame-retardant and smoke-suppressant mechanisms of different coatings.

Table 5
The compressive strength of EPS, EPS/10PF/3 EG and EPS/10PF/3AP.

Sample	EPS	EPS/10PF/3 EG	EPS/10PF/3AP
Compressive strength (kPa)	95 ± 5	202 ± 19	204 ± 17

Table 6
The thermal conductivities of EPS, EPS/10PF/3 EG and EPS/10PF/3AP.

Sample	EPS	EPS/10PF/3 EG	EPS/10PF/3AP
Thermal conductivity (W/m·K)	0.031	0.041	0.038

EPS/10PF/3AP is shown in Table 5. The compressive strength of neat EPS was only 95 kPa while that of EPS/10PF/3 EG and EPS/10PF/3AP was 202 and 204 kPa, respectively. It was showed that they were increased by 113% and 115%, respectively. The obvious increasement might be attributed to the hard shell formed by the flame-retardant coatings.

3.3.2. Thermal insulation property

Table 6 shows the thermal conductivities of neat EPS and the flame-retardant EPS composites. Thermal conductivity is one of the most important parameters to evaluate the thermal insulation for foams, which determines if the foam can be used as a thermal insulation material. Table 6 showed that neat EPS had a very low thermal conductivity of 0.031 W/m·K, and the values were increased to 0.041 W/m·K and 0.038 W/m·K for EPS/10PF/3 EG and EPS/10PF/3AP, respectively. It was noted that the values of EPS/10PF/3 EG and EPS/10PF/3AP remained at a comparative low level, which indicated the flame-retardant EPS composites were still good thermal insulation materials. More interestingly, the value of EPS/10PF/3AP was lower than that of EPS/10PF/3 EG, which could be ascribed to the good compatibility of PF and AP. There are a lot of hydroxyl in PF, which can form hydrogen bond with AP. While for EPS/PF/EG, there exists some cracks between PF and EG because of the large dimension of EG and no interaction between them.

4. Conclusion

Novel flame-retardant coating PF/AP and PF/EG were prepared to improve the flame retardancy and smoke suppression of EPS. The LOI and UL-94 tests results indicated that the coating improved the flame retardancy of EPS greatly and the flame-retardant efficiency of coating with AP was higher than the coating with EG. CC tests showed that the flame-retardant coatings could obviously decrease the TTI, PHRR and MLR values, demonstrating excellent flame retardancy. PSPR and TSP values revealed the coatings greatly suppressed the generation of the smoke during the combustion and improved the smoke suppression of EPS. It was notable that PF/AP coating endowed EPS with better flame-retardant and smoke-suppressant performances than PF/EG coating. The mechanism analysis by SEM, XPS, and Raman suggested that PF/AP could form a more compact P–O–C cross-linked char layer with better carbonaceous microstructure than PF/EG, resulting in better flame retardancy. Meanwhile, the coating with AP exhibited certain gas-phase activity due to the degradation of AP. The compressive strength of EPS composites was much higher than that of EPS, and the thermal conductivity of EPS composites remained at a comparative low level, which meant the flame-retardant EPS composites were still good thermal insulation materials. These above results show that the EPS composites have promising prospects in building thermal insulation field.

Novelty statement

An effective flame-retardant cell coating consisting of phenolic resin (PF) and aluminum hypophosphite (AP) was successfully designed and fabricated to endow expanded polystyrene (EPS) with excellent flame-retardant and smoke-suppressant performances. The PF reacting with AP by hydrogen-bond interaction forms a facile flame-retardant coating PF/AP, which not only greatly reduces flammability and smoke release, but also remains the thermal conductivities of EPS foams at low level. The large reduction in overall flammability and smoke release indicated EPS/PF/AP composites have enormous potential as building insulation materials. This work is useful for the development of highly fire-safety EPS.

Declaration of competing interest

The authors declare that they have no known competing financial interests or personal relationships that could have appeared to influence the work reported in this paper.

Acknowledgment

This work was financially supported by the National Natural Science Foundation of China (Grants 51827803, 51320105011, 51790504and 51721091), Young Elite Scientists Sponsorship Program by CAST, and Fundamental Research Funds for the central Universities.

Appendix A. Supplementary data

Supplementary data to this article can be found online at https://doi.org/10.1016/j.compositesb.2020.107797.

References

[1] Park HS, Oh BK, Cho T. Vibroacoustic behavior of full-scale sandwich floor with softened graphite-incorporated expanded polystyrene core. Compos B Eng 2018; 137:74–91.
[2] Yu Q, Zhao Y, Dong A, Li Y. Mechanical properties of EPS filled syntactic foams prepared by VARTM. Compos B Eng 2018;136:126–34.
[3] Caliskan U, Apalak MK. Low velocity bending impact behavior of foam core sandwich beams: experimental. Compos B Eng 2017;112:158–75.
[4] Park HS, Kim Y, Oh BK, Cho T. Compressive properties of graphite-embedded expanded polystyrene for vibroacoustic engineering applications. Compos B Eng 2016;93:252–64.
[5] Zhu ZM, Xu YJ, Liao W, Xu S, Wang YZ. Highly flame retardant expanded polystyrene foams from phosphorus–nitrogen–silicon synergistic adhesives. Ind Eng Chem Res 2017;56(16):4649–58.
[6] Jacob, E. US Patent 3058928, 1962.
[7] Stobby, W.G. US Patent WO9119758, 1991.
[8] Laoutid F, Bonnaud L, Alxandre M, Lopez-Cuesta JM, Dubois P. New prospect in flame retardant polymer material: from fundamentals to nanocomposites. Mater Sci Eng R 2009;63(3):100–25.
[9] Chen L, Wang YZ. A review on flame retardant technology in China. Part I: development of flame retardants. Polym Adv Technol 2010;21(1):1–26.
[10] Thoma H, Hauschultz G, Knorr E, Hutzinger O. Polybrominated dibenzofurans (PBDF) and dibenzodioxins (PBDD) from the pyrolysis of neat brominated diphenylethers, biphenyls and plastic mixtures of these compounds. Chemosphere 1987;16(1):277–85.
[11] Dumler R, Lenoir D, Thoma H, Hutzinger O. Thermal formation of polybrominated dibenzofurans from decabromodiphenyl ether in a polybutylene–terephthalate polymer matrix. J Anal Appl Pyrol 1989;16(2):153–8.
[12] Lu SY, Hamerton I. Recent developments in the chemistry of halogen–free flame retardant polymers. Prog Polym Sci 2002;27(8):1661–712.
[13] Li ME, Wang SX, Han LX, Yuan WJ, Cheng JB, Zhang AN, Zhao HB, Wang YZ. Hierarchically porous SiO_2/polyurethane foam composites towards excellent thermal insulating, flame-retardant and smoke-suppressant performances. J Hazard Mater 2019;375:61–9.
[14] Zhao HB, Chen M, Chen HB. Thermally insulating and flame-retardant polyaniline/pectin aerogels. ACS Sustainable Chem Eng 2017;5(8):7012–9.
[15] Jian RK, Ai YF, Xia L, Zhao LJ, Zhao HB. Single component phosphamide-based intumescent flame retardant with potential reactivity towards low flammability and smoke epoxy resins. J Hazard Mater 2019;371:529–39.
[[1][6] Zhao X, Zhang L, Alonso JP, Delgado S, Martínez-Miranda MR, Wang DY. Influence of phenylphosphonic amide on rheological, mechanical and flammable properties of carbon fiber/RTM6 composites. Compos B Eng 2018; 149:74–81.
[17] Elsabbagh A, Attia T, Ramzy A, Steuernagel L, Ziegmann G. Towards selection chart of flame retardants for natural fibre reinforced polypropylene composites. Compos Part B-Engineering 2018;141:1–8.

[18] Scarfato P, Incarnato L, Di Maio L, Dittrich B, Schartel B. Influence of a novel organo-silylated clay on the morphology, thermal and burning behavior of low density polyethylene composites. Compos B Eng 2016;98:444–52.
[19] Ran J, Qiu J, Xie H, Lai X, Li H, Zeng X. Combination effect of zirconium phosphate nanosheet and PU-coated carbon fiber on flame retardancy and thermal behavior of PA46/PPO alloy. Compos B Eng 2019;166:621–32.
[20] Kim JH, Kwon DJ, Shin PS, Baek YM, Park HS, DeVries KL, Park JM. The evaluation of the interfacial and flame retardant properties of glass fiber/unsaturated polyester composites with ammonium dihydrogen phosphate. Compos B Eng 2019;167:221–30.
[21] Kandola BK, Krishnan L, Ebdon JR. Blends of unsaturated polyester and phenolic resins for application as fire-resistant matrices in fibre-reinforced composites: effects of added flame retardants. Polym Degrad Stabil 2014;106:129–37.
[22] Glueck G, Dietzen FJ, Hahn K, Ehrman G, to BASF. PCT patent WO 00/34342. 2000.
[23] Dietzen FJ, Glueck G, Ehrman G, et, al, to BASF, US Patent 6420442, 2002.
[24] Hahn K, Ehrman G, Ruch J, Schmied B, to BASF, PCT Patent 06/058734, 2006.
[25] Yan YW, Huang JQ, Guan YH, Wang YZ. Flame retardance and thermal degradation mechanism of polystyrene modified with aluminum hypophosphite. Polym Degrad Stabil 2014;99:32–45.
[26] Zhao B, Chen L, Long JW, Wang YZ. Aluminum hypophosphite versus alkyl-substituted phosphinate in polyamide 6: flame retardance, thermal degradation, and pyrolysis behavior. Ind Eng Chem Res 2013;52(8):2875–86.
[27] Everest DA. Aluminum hypophosphite. J Chem Soc 1952;7. 2945-5.
[28] Bakhtiyari S, Taghi-Akbari L, Ashtiani MJ. Evaluation of thermal fire hazard of 10 polymeric building materials and proposing a classification method based on cone calorimeter results. Fire Mater 2015;39(1):1–13.
[29] Wang DY, Liu Y, Wang YZ, Artiles CP, Hull TR, Price D. Fire retardancy of a reactively extruded intumescent flame retardant polyethylene system enhanced by metal chelates. Polym Degrad Stabil 2007;92(8):1592–8.
[30] Rao WH, Liao W, Wang H, Zhao HB, Wang YZ. Flame-retardant and smoke-suppressant flexible polyurethane foams based on reactive phosphorus-containing polyol and expandable graphite. J Hazard Mater 2018;360:651–60.
[31] Shang K, Liao W, Wang YZ. Thermally stable and flame-retardant poly (vinyl alcohol)/montmorillonite aerogel via a facile heat treatment. Chin Chem Lett 2018;29(3):433–6.
[32] Breulet H, Steenhuizen T. Fire testing of cables: comparison of SBI with FIPEC/Europacable tests. Polym Degrad Stabil 2005;88(1):150–8.
[33] Horrocks AR. Textile flammability research since 1980- Personal challenges and partial solutions. Polym Degrad Stabil 2013;98(12):2813–24.
[34] Zhou K, Zhang Q, Liu J, Wang B, Jiang S, Shi Y, Gui Z. Synergetic effect of ferrocene and MoS2 in polystyrene composites with enhanced thermal stability, flame retardant and smoke suppression properties. RSC Adv 2014;4(26):13205–14.
[35] Liu XQ, Wang DY, Wang XL, Chen L, Wang YZ. Synthesis of functionalizedα-zirconium phosphate modified with intumescent flame retardant and its application in poly(lactic acid). Polym Degrad Stabil 2013;98(9):1731–7.
[36] Sadezky A, Muckenhuber H, Grothe H, Niessner R. Raman microspectroscopy of soot and related carbonaceous materials: spectral analysis and structural information. Carbon 2005;43(8):1731–42.
[37] Zhao HB, Cheng JB, Zhu JY, Wang YZ. Ultralight CoNi/rGO aerogels toward excellent microwave absorption at ultrathin thickness. J Mater Chem C 2019;7(2):441–8.
[38] Tai QL, Hu Y, Yuen RKK, Song L, Lu HD. Synthesis, structure–property relationships of polyphosphoramides with high char residues. J Mater Chem 2011;21(18):6621–7.
[39] Tuinstra F, Koening JL. Raman spectrum of graphite. J Chem Phys 1970;53(3):1126–30.
[40] Ferrari AC, Robertson J. Interpretation of Raman spectra of disordered and amorphous carbon. Phys Rev B 2000;61(20):14095–107.
[41] Bourbigot S, Le Bras M, Delobel R, Decressain R, Amoureux JP. Synergistic effect of zeolite in an intumescence process: study of the carbonaceous structures using solid-state NMR. J Chem Soc Faraday Trans 1996;92(1):149–58.
[42] Hu S, Song L, Pan HF, Hu Y. Thermal properties and combustion behaviors of chitosan based flame retardant combining phosphorus and nickel. Ind Eng Chem Res 2012;51(9):3663–9.